

ESTIMATION OF COSEISMIC DISPLACEMENT IN THE 2016 KUMAMOTO EARTHQUAKE FROM LIDAR DATA

Luis MOYA, Fumio YAMAZAKI, Wen LIU, and Tatsuro CHIBA

ABSTRACT: The geodetic displacement produced in the near field of the Mw7.1 Kumamoto earthquake was calculated from a pair of digital surface models, before and after the earthquake, obtained from airborne LIDAR data. A window matching search approach based on the correlation coefficient between the two images was used for this purpose. Besides, the results are compared and validated with the geodetic displacement calculated from strong-motion records. Furthermore, our results delineate the fault line, which is consistent with the surveyed active faults in Japan.

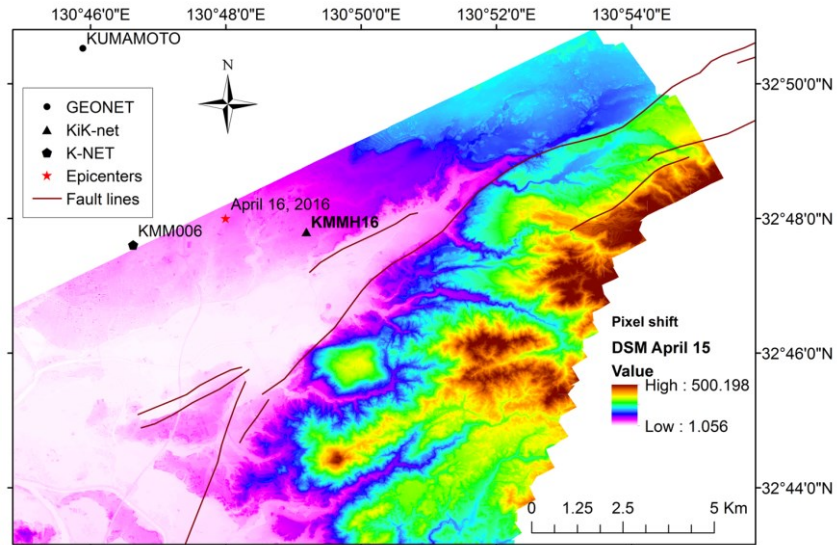
KEYWORDS: geodetic displacement; LIDAR; the 2016 Kumamoto earthquake; acceleration record

1. INTRODUCTION

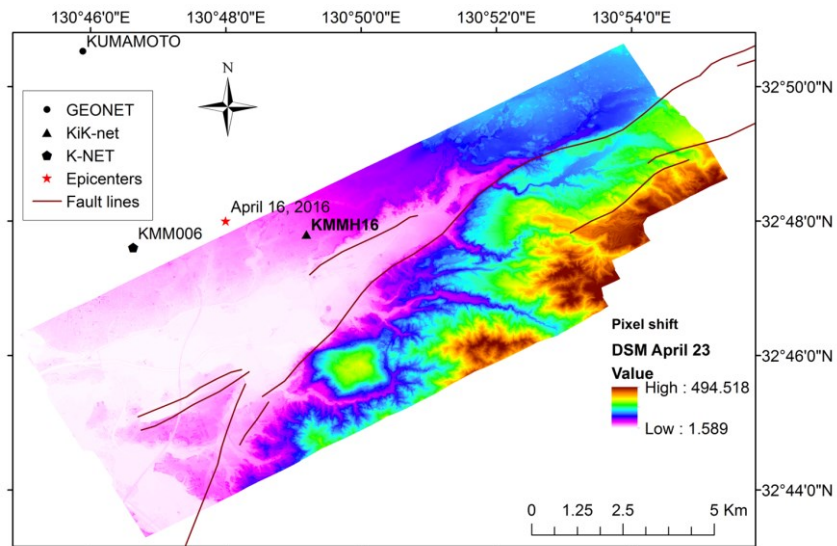
On April 14, 2016 at 21:26 an Mw6.5 earthquake occurred in Kumamoto prefecture, Japan. The epicenter (32.7°N, 130.8°E and 11 km depth) was located at the end of the Hinagu fault. About 28 hours later (April 16, 2016 at 01:25), another earthquake of Mw7.1 occurred in the Futagawa fault. Thus the first event was designated as the "foreshock" and the second one as the "mainshock". The both events were located in the suburban area of Kumamoto city with 735 thousand population. Therefore, extensive damage such as human loss, collapse of buildings and bridges, landslides, damage to soils and foundations, and damage of historical structures occurred.

Light Detection And Ranging (LIDAR) has many applications in earthquake engineering, such as surface deformation and landslide detection (Muller and Harding 2007, Kayen et al. 2006, Nissen et al. 2012, Duffly et al. 2013, Oskin et al. 2012). LIDAR technology uses pulses of laser light towards the ground and records the return time of each pulse to calculate the distance between the sensor and several surfaces above the ground (Lillesand et al. 2004).

This paper shows an estimation of the permanent surface displacement due to the mainshock of the Kumamoto earthquake calculated from the Digital Surface Models (DSM) obtained from LIDAR flights. In this case study a pair of DSM's is available: one just after the foreshock (on April 15) and one after the mainshock (April 23). We also compare our results with the permanent ground displacement estimated from an acceleration record obtained by the KiK-net system.



(a)



(b)

Figure 1. (a) the pre-event DSM and (b) the post-event DSM obtained from LIDAR

2. DATA DESCRIPTION

2.1 Digital Surface Model

On April 15, 2016, one day after the big foreshock, a LIDAR DSM was collected by Asia Air Survey Co., Ltd., in order to record the surface rupture and the building damage produced by the earthquake. The survey generated a ground return densities averaging 1.5~2 points/m². However, due to the unexpected mainshock of Mw7.1 occurred on April 16, a second mission to acquire LIDAR data was sent on April 23, which was able to generate average point densities of 3~4 points/m². This dataset is one of the few cases in which pre- and post-event DSMs are available with the same airplane, instrument, and

pilot (Air Survey Co., Ltd. 2016). For the sake of brevity, we will refer the DSM collected on April 15 and April 23 as the pre-event DSM and post-event DSM, respectively. After rasterize the raw point clouds, the DSMs have a data spacing of 50 cm and were registered in the Japan Plane Rectangular Coordinate System through the same preprocessing procedure.

Figure 1 shows the extension of the pre- and post-event DSMs, where it can be observed that the pre-event DSM extends a bigger area than the post-event DSM does. The common area from the both DSMs covers parts of the Mashiki town, Kashima town, Mifune town, and Nishihara village. The whole common area is composed of rural residential areas, agricultural fields and forests. The common area also includes a part of the Futagawa fault, which caused the mainshock of the Kumamoto earthquake.

2.2 Strong motion accelerations

Inside the scene, a station (KMMH16 in the Mashiki town) that belongs to the KiK-net, one of the biggest strong-motion network in Japan, is located (**Figure 1**). In the Kik-net, two 3-component accelerometers are placed on the ground surface and in the borehole at the base-rock level. At the Mashiki station, the borehole accelerometer was placed at -255 meter from the ground surface in the bedrock.

Figure 2 shows the acceleration, velocity and displacement time histories after applying a baseline correction proposed by Moya et al. (2016). A permanent displacement with 100 cm, 50 cm, and 55 cm was observed toward the east, north, and downward, respectively. Note in this joint inversion approach, the common permanent displacement can be obtained for the two accelerometers. It is noted that the surface acceleration was much bigger (amplified) than the baserock one, the displacements reached the same value both on the surface and in the bedrock.

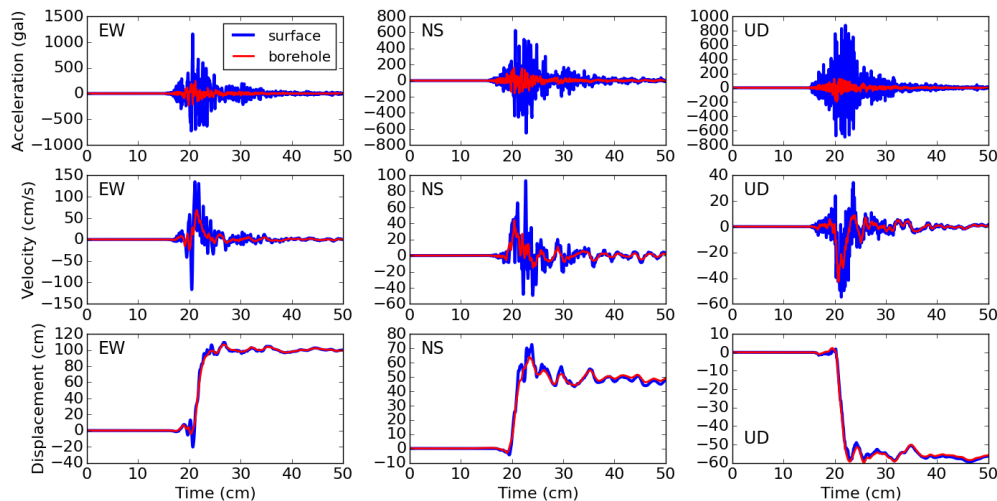


Figure 2. Acceleration, velocity and displacement time histories after removing the shift in the velocity record for the mainshock recorded at the KiK-net Mashiki (KMMH16) station on the ground surface and in the borehole.

3. METHODOLOGY TO ESTIMATE THE PERMANENT DISPLACEMENT

To construct the coseismic displacement distribution in space, we perform a matching search by using a moving window of the post-event DSM on the surrounded area of the pre-event DSM. We use the correlation coefficient to identify the best matching location between the two DSMs. The shift detected between the two matched windows is estimated as the coseismic displacement. The similar approach was employed for optical satellite images in vehicle location matching (Liu et al. 2011) and for SAR intensity data in building location matching (Liu et al. 2013).

Due to the spatial-resolution (pixel spacing) of the LIDAR data, we can only estimate the displacement with multiples of 50 cm. In order to illustrate the approach, we selected an area close to the KiK-net Mashiki station (**Figure 3a**) so that we can compare our results with the coseismic displacement from the acceleration record in the KiK-net station. **Figure 3c** shows 61 x 61 pixel window of the post-event DSM and **Figure 3b** shows a 101x101 pixel window of the pre-event DSM. The pixel located at the center of the two windows has the same spatial coordinates.

Figure 4 shows the correlation coefficient calculated from a moving window of **Figure 3c** within **Figure 3b**. The location of the maximum value relative to the center of the window is two pixels to the west and one pixel to the south, which is interpreted as a coseismic displacement of 100 cm eastward and 50 cm northward. Our results are consistent with the displacement time history calculated from the acceleration records (**Figure 2**).

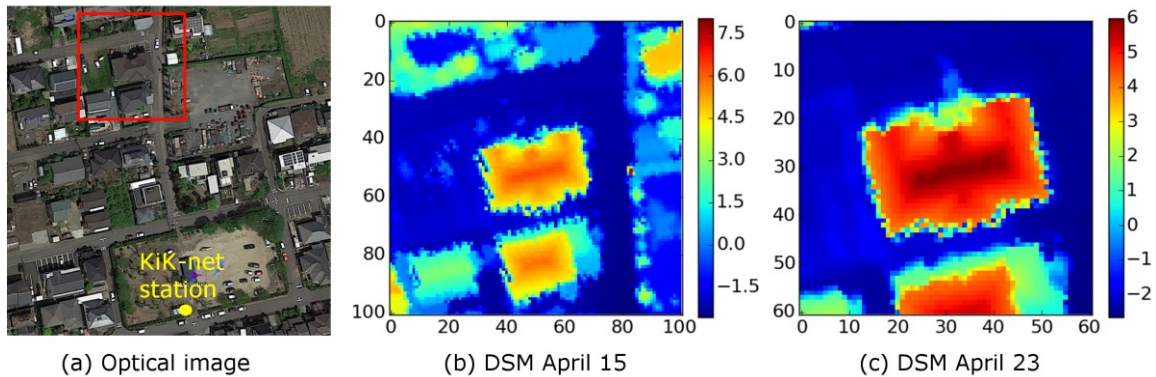


Figure 3. (a) An example of the matching technique. (b) The DSM taken on April 15 located in the red rectangle in (a). (c) The DSM taken on April 23 located within the red rectangle in (a).

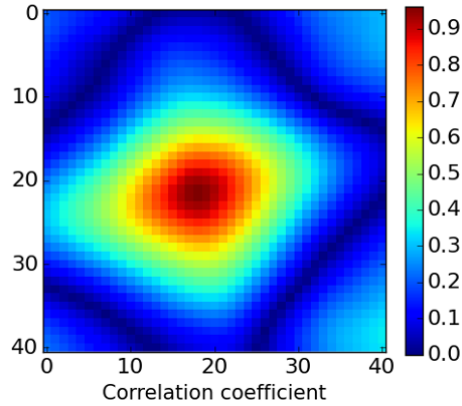


Figure 4. Distribution of the correlation coefficient value between the two DMSs used to estimate the permanent displacement

The east-west component of the coseismic displacement calculated from the approach mentioned is shown in **Figure 5**. The result shows a low level of noise that is called salt-and-pepper noise in the image processing community. The white pixels are mostly due to the loss of information (matching data) in the elevation of the DSMs. The median filter, calculated with window size 5x5, was introduced to remove the noise.

The obtained result for the horizontal displacement is shown in the east-west component (**Figure 6a**) and in the north-south component (**Figure 6b**). The change of direction of the coseismic displacement, in both components, delineates the Futugawa fault line which is consistent with the surveyed active faults in Japan (Geological Survey Institute of Japan 2016). In the east-west component, a displacement of 1.5 m (to the east) was detected in the northern area and 0.5 m (to the west) in the souther area of the fault line. In the north-south component, a displacement of 0.5 m (to the north) was detected in the northern area and 1.0 m (to the south) in the souther area of the fault line. The trend of the crustal movement is consistent with the result of SAR interferometry using ALOS-2 PALSAR-2 imagery (Geospatial Information Authority of Japan 2016).

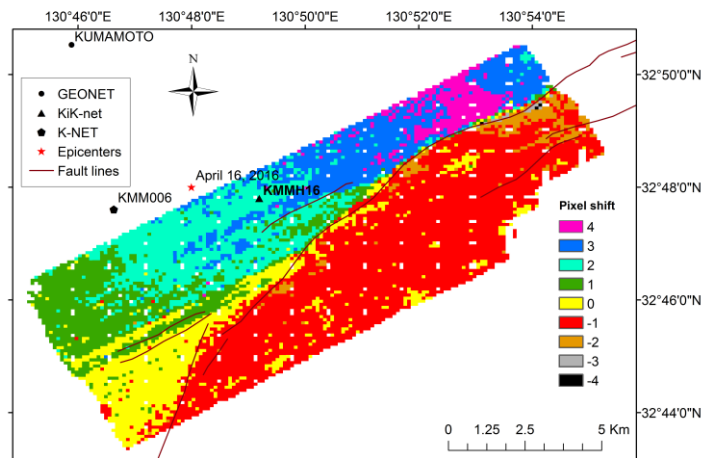
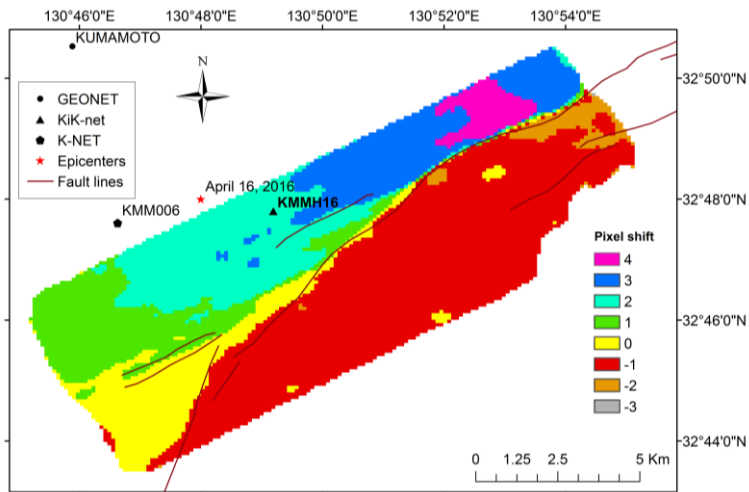
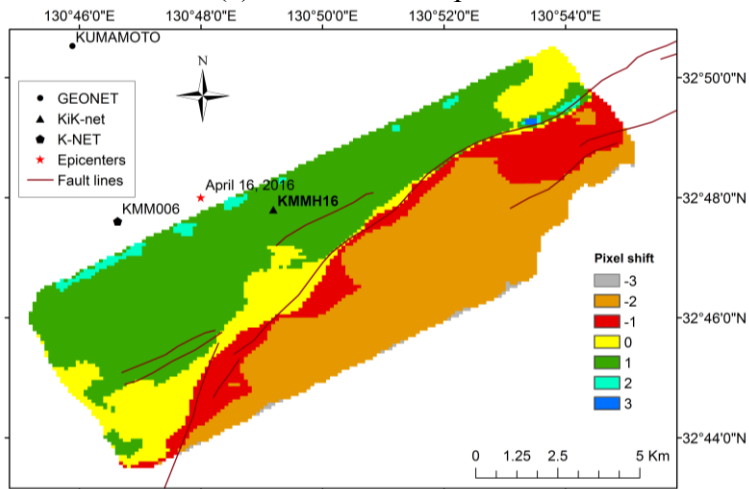


Figure 5. East-west component of the coseismic displacement calculated from the DSMs



(a) East-West component



(b) North-South component

Figure 6. Permanent ground displacement after applying the median filter.

4. CONCLUSIONS

The crustal movement in the period after the 14 April foreshock was estimated using two DSMs collected by LIDAR flights before and after the 16 April mainshock of the Mw7.1 Kumamoto earthquake. The correlation coefficient was used in a window matching technique between the two DSMs in order to calculate the permanent ground displacement. The results show good agreement with the permanent displacement calculated from acceleration records and with the Futugawa fault line published previously. The spatial distribution of the displacement may be used in assessing the mechanism of the Kumamoto earthquake sequence and evaluating the strong motion distribution along the fault line.

REFERENCES

- Asia Air Survey Co., Ltd. (2016) 2016 Kumamoto Earthquake.
<http://www.ajiko.co.jp/en/blog/y2016/id572751JWX/>
- Duffy, B., Quigley, M., Barrel, D. J. A., Dissen, R. V., Stahl, T., Leprince, S., cInnes, C., and Bilderback, E. (2013) Fault kinematics and surface deformation across a releasing bend during the 2010 Mw 7.1 Darfield, New Zealand, earthquake revealed by differential LiDAR and cadastral surveying. **Geological Society of America Bulletin**, Vol 125, No. 3/4, 420-431.
- Geological Survey Institute of Japan (2016) Kumamoto Earthquakes 2016 information.
<https://www.gsj.jp/en/hazards/kumamoto2016/index.html>
- Geospatial Information Authority of Japan (2016) the Kumamoto Earthquake.
<http://www.gsi.go.jp/BOUSAI/H27-kumamoto-earthquake-index.html#3>
- Kayen, R., Collins, B. D., Bawden, G., and Pack, R. T. (2006) Earthquake deformation analysis using terrestrial scanning Laser-LIDAR technology. **Proceedings of the 8th U.S. National Conference on Earthquake Engineering**, San Francisco, April 18-22, 10 pages
- Lillesand, T. M., Kiefer, R. W., and Chipman, J. W. (2004) **Remote Sensing and Image Interpretation**. 5th ed. John Wiley and Sons, Inc.: United States.
- Liu, W., Yamazaki, F., and Vu, T.T. (2011) Automated Vehicle Extraction and Speed Determination from QuickBird Satellite Images. **Journal of Selected Topics in Applied Earth Observations and Remote Sensing**, IEEE, Vol. 4, No. 1, 75-82.
- Liu, W., and Yamazaki, F. (2013) Detection of Crustal Movement from TerraSAR-X intensity images for the 2011 Tohoku, Japan Earthquake. **Geoscience and Remote Sensing Letters**, IEEE, Vol. 10, No. 1, 199-203.
- Moya, L., Yamazaki, F., and Liu, W. (2016) Comparison of coseismic displacement obtained from GEONET and seismic networks. **Journal of Earthquake and Tsunami**, Vol. 10, No. 2, pp. 1640002-1-18, doi: 10.1142/S1793431116400029.
- Muller, J. R., and Harding, D. J. (2007) Using LIDAR surface deformation mapping to constrain earthquake magnitudes on the seattle fault in Washington state, USA. **Urban Remote Sensing Joint Event, IEEE**, 7 pages.
- Nissen, E., Krishnan, A. K., Arrowsmith, J. R., and Saripalli, S. (2012) Three-dimensional surface displacement and rotations from differencing pre- and post-earthquake LiDAR point clouds. **Geophysical Research Letters**, Vol 39, L12301, 6 pages.
- Oskin, M. E., Arrowsmith, J. R., Corona, A. H., Elliot, A. J., Fletcher, J. M., Fielding, E. J., Gold, P. O., Garcia, J. G., Hudnut, K. W., Liu-Zeng, J., and Teran, O. J. (2012) Near-field deformation from the El Mayor-Cucapah earthquake revealed by differential LIDAR. **Science**, Vol. 335 (6069), 702-705.

ABOUT THE AUTHORS

Luis Moya is a PhD candidate at the Department of Urban Environment Systems, Chiba University, Japan. E-mail: lmoyah@chiba-u.jp

Fumio Yamazaki is a professor at the Department of Urban Environment Systems, Chiba University, Japan. Email: fumio.yamazaki@faculty.chiba-u.jp

Wen Liu is an assistant professor at the Department of Urban Environment Systems, Chiba University, Japan. Email: wen.liu@chiba-u.jp

Tatsuro Chiba is Chief Engineer at the Research and Development Institute, Asia Air Survey Co., Ltd., Japan. Email: ta.chiba@ajiko.co.jp

ACKNOWLEDGEMENTS

The LIDAR data used in this study were acquired and owned by Asia Air Survey Co., Ltd., Japan. We also thank the National Research Institute for Earth Science and Disaster Prevention (NIED) for providing the acceleration record of Mashiki KiK-net station.